2024 IEEE/ASME International Conference on Advanced Intelligent Mechatronics (AIM)
July 15-19, 2024. Boston, MA, USA

A transparent spherical microscope stage to realize tracking and omni-directional imaging with 6 degrees of freedom*

Josephine Galipon, Aymeric Bordier, Maxime Duby, Moses Gladson Selvamuthu, Makishi Imaizumi, Riichiro Tadakuma, and Kenjiro Tadakuma, *Member, IEEE*

***Abstract*— To achieve an observation stage with 6 degrees of freedom, a specimen was placed at the center of a transparent sphere or polyhedron. This novel configuration enables not only positional tracking, but also posture tracking, as well as scanning on three rotational axes. After discussing the solution space for spherical and polyhedral shapes and the mechanisms available to achieve 6-DoF, we demonstrate our invention with two proof-of-concept prototypes: (1) the polyhedron-gimbal, which allows simultaneous rotation of pitch, yaw, and roll, and (2) an actuated sphere-retractable axis version, which uses friction for pitch and roll, and a gear mechanism for yaw. To the best of our knowledge, this is the first example of omni-directional imaging suitable for 3D stereomicroscopy of biological organisms. In the future, it will be applied to the monitoring of 3D cellular growth in various conditions.**

***Video abstract*— https://youtu.be/kJLVPvKqaOc**

I. Introduction

The goal of this study is the development of an optical stereomicroscope that can handle not only positional tracking, but also multi-directional imaging, and 3D reconstruction of a live specimen. Microscopy has a long history dating back to the 17th century [1]. In terms of tracking living organisms, an actuated XY stage was developed to track motile microorganisms [2]. This was expanded in the Z direction [3], and the specimen could be followed in 3D space. Finally, a vertical tracking microscope enables the tracking of swimming plankton over one infinitely rotating axis [4]. In all of these systems, tracking is the main purpose, and the freely-moving organism may face the observer from any direction. Other systems allow 3D scanning, for example by fixing a specimen in a rotating cylinder, combined with light sheet fluorescence microscopy (LSFM), but the top and bottom of the sample is difficult to resolve and limited to sub-millimeter transparent samples [5].

To achieve both posture-tracking and multi-directional imaging, we achieved the proof of principle of a microscope stage with six degrees of freedom (6-DoF) by positioning the specimen on the inside of a transparent polyhedron or sphere. To our knowledge, this is the first concept of microscope stage capable of three linear and three rotational axes. Depending on the nature of the specimen, the spherical stage enables various analyses ranging from positional tracking to multi-directional imaging and the reconstruction of 3D models. In this paper, we present and discuss the following first two prototypes:

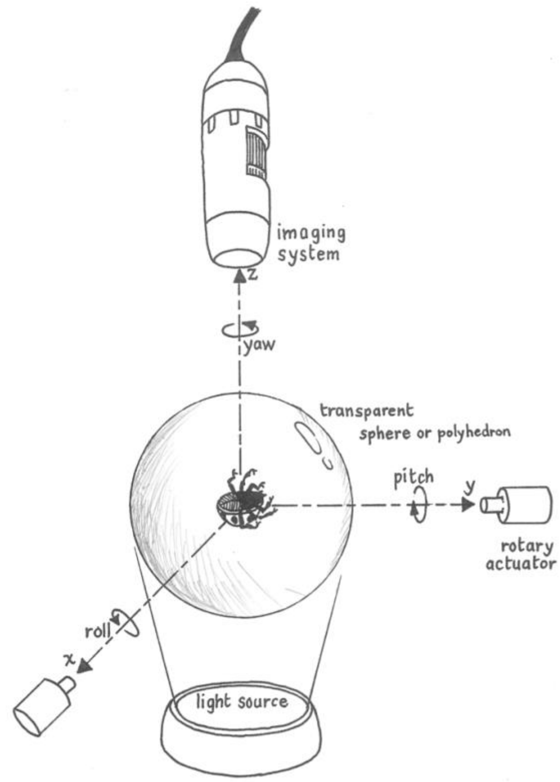

Figure 1. Representation of the basic principle for the 6-DoF spherical microscope stage. The type and position of the light source and imaging system may vary [6].

(1) Polyhedral stage with gimbal mechanism. This configuration allows multi-angle imaging of either immobile or slowly-growing structures, demonstrating the feasibility of the concept.

(2) Spherical stage with retractable pitch and roll axes based on a friction mechanism. This *configuration* can achieve tracking, multi-angle imaging, and 3D scanning.

*Research supported by The Japan Keirin Autorace (JKA) Foundation, 2023M-254 and 2024M-527. A patent sponsored by Keio University (2022-140257) was filed.

J.G. Author is with Yamagata University, Yonezawa, 992-8510, Japan and Keio University, Tsuruoka, 997-0035 (corresponding author to provide phone: +81(0)238-26-3216; e-mail: jgalipon@yz.yamagata-u.ac.jp).

A. B. and M. D. Authors were with Yamagata University, Yonezawa, 992-8510, Japan and ESEO, Angers, 49000, France, and are now affiliated with the latter (e-mails: aymeric.bordier & maxime.duby@reseau.eseo.fr).

M. G. S., M. I., and R. T. Authors are with Yamagata University, 992-8510, Japan (e-mails: t236823d & t223114m@st.yamagata-u.ac.jp & tadakuma@yz.yamagata-u.ac.jp).

K. T. is with Tohoku University, Sendai, 980-8579, and is currently at Osaka University, Japan (email: kenjiro.tadakuma.es@osaka-u.ac.jp).

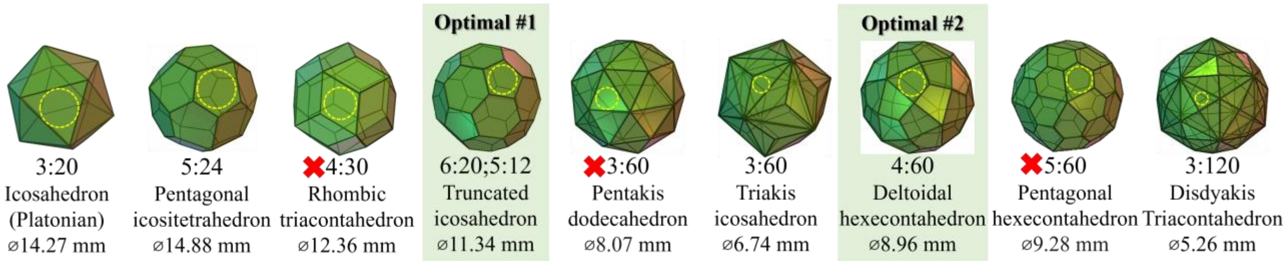

Figure 2. A selection of possible configurations for the polyhedral stage. The yellow circle indicates the inner circle of the smallest face. The diameter of this inner circle is indicated for each polygon assuming an equal mid-sphere radius of 20 mm. Values calculated using formulas available on rechneronline.de [7]; polyhedral representations were obtained from Wikicommons.

This paper aims not only to establish the proof of principle for this invention and to comprehensively discuss the solution space for possible embodiments and their applications.

II. Mechanism Principle

A. Ideal case

The core principle is illustrated in **Fig. 1**. In addition to the common translational movements along the X, Y, and Z axes found in standard microscopes, pitch, roll, and yaw rotational axes are added to enable full freedom to observe the specimen from any angle. To enable this, the position of the specimen is either fixed at the center of a transparent sphere or polyhedron, allowing for posture-tracking and 360° imaging over all three rotational axes, or the specimen is allowed to walk or crawl on the inner part of the sphere, which then represents an infinite surface for positional tracking. Imaging is then achieved by appropriately positioning one or more light sources and one or more imaging devices. Although the present study focuses on optical microscopy, in theory, this principle will work with a wide variety of imaging devices not limited to microscopy.

B. Solution space: which polyhedron?

By allowing maximum freedom in terms of vision angles, the spherical configuration is the ideal case in theory. However, major challenges are to be faced when designing a spherical transparent stage: (1) how to manufacture a perfect sphere that both transparent and hollow, considering that any imperfection will create a dead angle which will interfere with either image acquisition, or the rotation mechanism, or both? (2) if any lens distortion were to occur due to the curvature of the sphere, it would be necessary to add some kind of optical corrective lens or lens distortion correction image processing, which can add distance from the lens to the subject resulting in a darker image and/or loss of resolution, or slower processing.

If a sphere is cut into a polyhedron with opposite faces that are parallel to each other, light distortion should be minimized. In addition, a hollow polyhedron with transparent faces should be easier to manufacture than the hollow sphere. As a tradeoff, the following two limitations occur: (1) the number of angles available for multi-angle imaging is limited by the number of faces of the polyhedron; (2) in case the experimenter wishes to observe the whole sample, the size of the sample that may be observed is limited by the diameter of the inner circle of the smallest face of the polyhedral.

Fig. 2 shows a lineup of nine polyhedra with characteristics relevant to this study. Among these, two configurations were considered optimal for maximizing sample size and number of faces: the deltoidal hexecontahydron (4:60, sixty deltoidal faces) with the faces' inner circle diameter of 8.96 {mm}, and the truncated icosahedron (6:20;5:12, 6 hexagonal and 12 pentagonal faces), otherwise known as buckminsterfullerene C_{60}, also known as the "buckyball" or "soccer ball", with the smallest faces' inner circle diameter being 11.34 {mm} [8,9]. We can see here that despite the clear tradeoff between maximum sample (or specimen) size and the number of faces, faces with bigger inner circles tend to be more desirable in to achieve a wider field of vision.

To confirm whether the opposite faces are parallel to each other, these polygons were 3D printed and tested manually, as can be seen in **Fig. 3**, by using a level gauge. Polyhedra which do not fit this requirement have a red cross mark in **Fig. 2**.

The faces' inner circle diameters indicated in **Fig. 2** assume zero thickness for the edges, but one must take into account the thickness of the skeleton structure that is manufactured. To

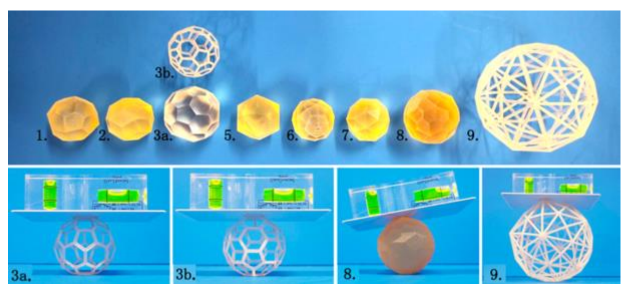

Figure 3. Method for testing whether the opposite faces of the polyhedra are parallel using a level gauge. 1. Pentagonal icositetrahedron (5:24), 2. Rhombic triacontahedron (4:30), 3. Truncated icosahedron (6:20;5:12), 5. Triakis icosahedron (3:60), 6. Deltoidal hexecontahedron (4:60), 7: Pentakis dodecahedron (3:60), 8: Pentagonal hexecontahedron (5:60); 9: Disdyakis triacontahedron (3:120) [6].

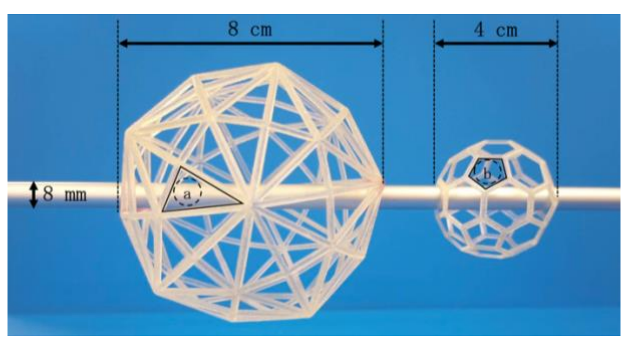

Figure 4. Comparison of the 3D printed skeleton of (3:120) polyhedron on the left with the "soccer ball" polyhedron on the right, when the faces' inner circles diameters are a = b = 8 {mm} [6].

experimentally confirm the target specimen size, the fullerene C_{60} (32 faces) and the disdyakis triacontahedron (120 faces) were 3D printed so that the inner circle diameter is 8 {mm} in both cases. As seen in **Fig. 4**, the cross-section's diameter was approximately 40 {mm} for the fullerene C_{60} and 80 {mm} for the disdyakis triacontahedron, the latter too large of a working distance for most stereomicroscopes. This value of 40 {mm} corresponds to the theory presented in Fig. 2 as all calculations were done for a mid-sphere radius of 20 {mm}. In practice, 2-3 millimeters should be removed from the values presented in **Fig. 2**.

In this study, two prototypes are presented as a proof of concept for the 6-DoF omni-directional microscope stage:

(A) the fullerene C_{60} or "soccer ball" configuration;

(B) the spherical configuration.

C. Configuration of the rotational axes

Several mechanisms can enable the rotation of a sphere or polyhedron on the roll, pitch, and yaw axes. The two best candidates for our system are presented in **Fig. 5**. The gimbal in **Fig. 5(a)** enables simultaneous rotation on all three axes, but at the expense of introducing some dead angles and increasing the distance from the microscope lens or camera. In addition, no gear mechanism may be placed inside the sphere as it would impede observation [10]. In practice, this means that it is will be difficult to actuate, and but suitable for manual manipulation. This configuration may be useful for rapid simultaneous multi-angle imaging by using a set of imaging devices positioned at several angles.

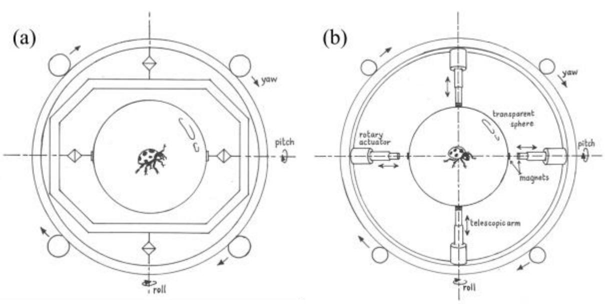

Figure 5. Suitable mechanisms for rotating the transparent sphere over three axis with maximum visibility of the observed specimen [6].

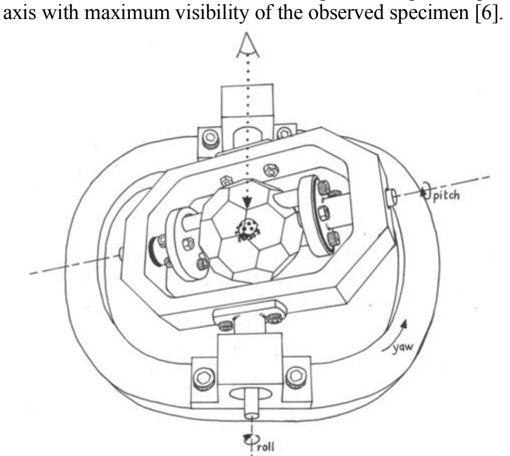

Figure 6. Design of the proof-of-concept prototype for the polyhedron-gimbal configuration [6].

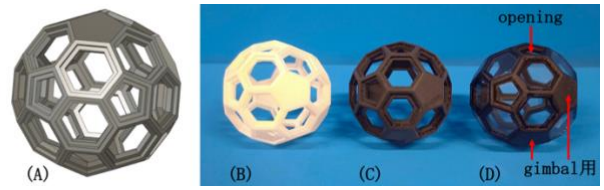

Figure 7. Steps for building the polyhedral microscope stage [6].

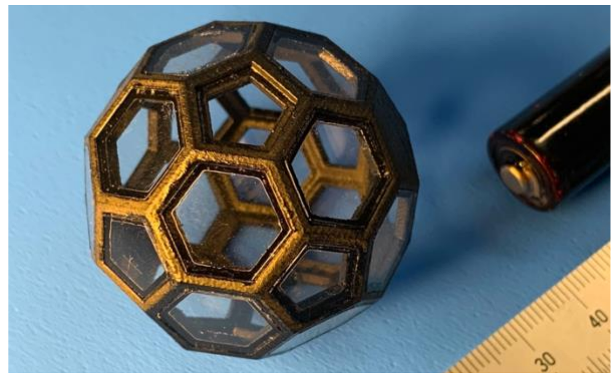

Figure 8. Polyhedral microscope stage ready to use [6].

The second candidate we selected is the friction or magnetic-based mechanism placed at the end of retractable arms for the pitch and roll axes, in combination with a gear for the yaw axis, as shown in **Fig. 5(b)**. In this case, the yaw, pitch, and roll axis can be actuated, and the total range of observable angles is higher, at the expense of having to rotate the axes one by one. This configuration may be useful for 3D scanning by acquiring a series of images along each rotational axis, for the monitoring of slowly-growing structures such as plant seed germination, embryos, or 3D cell cultures, and for live tracking.

While other mechanisms may be possible, such as using various types of omni-foil wheels [11,12], or perhaps even a partially transparent version of the omni-directional spherical gear [13], the limitations are more severe, in controllability and traceability of the rotational coordinates in the former, and with the introduction of gear backlash and teeth interfering with light diffraction for the latter.

In this paper, we present two initial prototypes as proof of concepts for the mechanisms selected in **Fig. 5**:

(A) Combination of "soccer ball" polyhedron and gimbal;

(B) Combination of transparent sphere and retractable roll and pitch axes based on friction, and a yaw axis gear, with actuation.

III. First Prototype: Polyhedron & Gimbal

As an initial proof of concept, we built a fullerene C60 with transparent faces and set it on a gimbal as shown in **Fig. 6**.

A. Prototype building

A truncated icosahedron frame with a largest cross-section of 40 {mm} and a 1 {mm} indentation was created in Fusion 360 as in **Fig. 7(a)**. After printing with the high-resolution 3D printer AGILISTA-3100, the model was coated with matte black spray paint as in **Fig. 7(b)** and **Fig. 7(c)**. Then, pentagons and hexagons were cut from 1 {mm}-thick transparent acrylic sheets using a laser cutter, and then adhered to the model with Konishi Co., Ltd.'s Aron Alpha Tough Power as in **Fig. 7(d)**. Two of the faces on each side were designed as filled from the beginning to fix the gimbal axis. Also, one of the pentagon faces was initially left open to allow for insertion of the sample or specimen and to allow filling with a transparent gel. Leaks were checked by enclosing water.

Finally, the gimbal axes were designed in Pro ENGINEER, printed using AGILISTA-3100, and assembled using stainless parts to allow for fixing and rotating. The whole system was mounted onto an aluminum frame which represents the XYZ stage and yaw axis. The latter are assumed to be feasible at this stage, as the purpose of this initial prototype is to validate the use of a transparent polyhedron as a means to observe a sample from many angles. Therefore, we chose to focus on the pitch and roll axes at first.

B. Prototype evaluation

A common spider with a body length of 5 {mm}, from the species *Yaginumia sia*, was collected on Aobayama campus, and subjected to freezing temperatures for two hours (**Fig. 10**). In the meantime, the polyhedron was half-filled with 4 % (w/v) agar from Matsuki Agar Industrial Co., Ltd. Subsequently, the spider was pre-encapsulated in a small amount of agar to avoid damaging any body parts. This agar-incrusted spider was then gently placed in the middle of the stage, which was further filled with more agar. Care was taken to ensure that no bubbles entered as the remaining space was filled. The final prototype with the polyhedral observation stage mounted onto the gimbal can be seen in **Fig. 11**. Before mounting it onto the gimbal, the specimen was confirmed to be positioned at the center of the polyhedron by observing from all directions as in **Fig. 12**.

Figure 10. Spider specimen used for prototype testing [6].

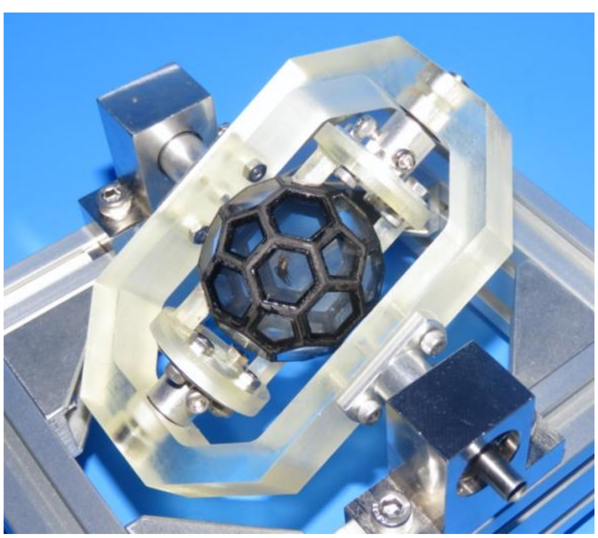

Figure 11. Final prototype for the polyhedron-gimbal [6].

Figure 12. Specimen at the center of the polyhedron, seen from various angles [partially from 6]. The pictures were acquired using an ordinary camera. The two pictures at the bottom are the zoomed-in versions of the first two pictures in the first row. Scale bar 2 {mm}.

Next, a USB hand-held microscope was used to acquire higher resolution pictures from 26 angles (**Fig. 13**), demonstrating the mechanism. Some details such as hairs on the spider's body could be observed from various angles.

IV. Second Prototype: Transparent Sphere & Actuated Retractable Axes

To further demonstrate the feasibility and applications of our invention, we developed a second prototype which takes advantage of the spherical configuration. At the same time, to avoid the bulkiness of the gimbal mechanism and make it easy to use with a wide range of stereomicroscopes, we designed retractable pitch and roll axes that can rotate the sphere using a friction mechanism. The sphere is fixed using a system of eight 4 {mm}-diameter caster balls (four on top, four at the bottom) to prevent the sphere from shifting when the working axis exerts pressure onto it. **Fig. 14** shows a schematic representation of the entire mechanism, while **Fig. 15** shows the detail of the yaw axis.

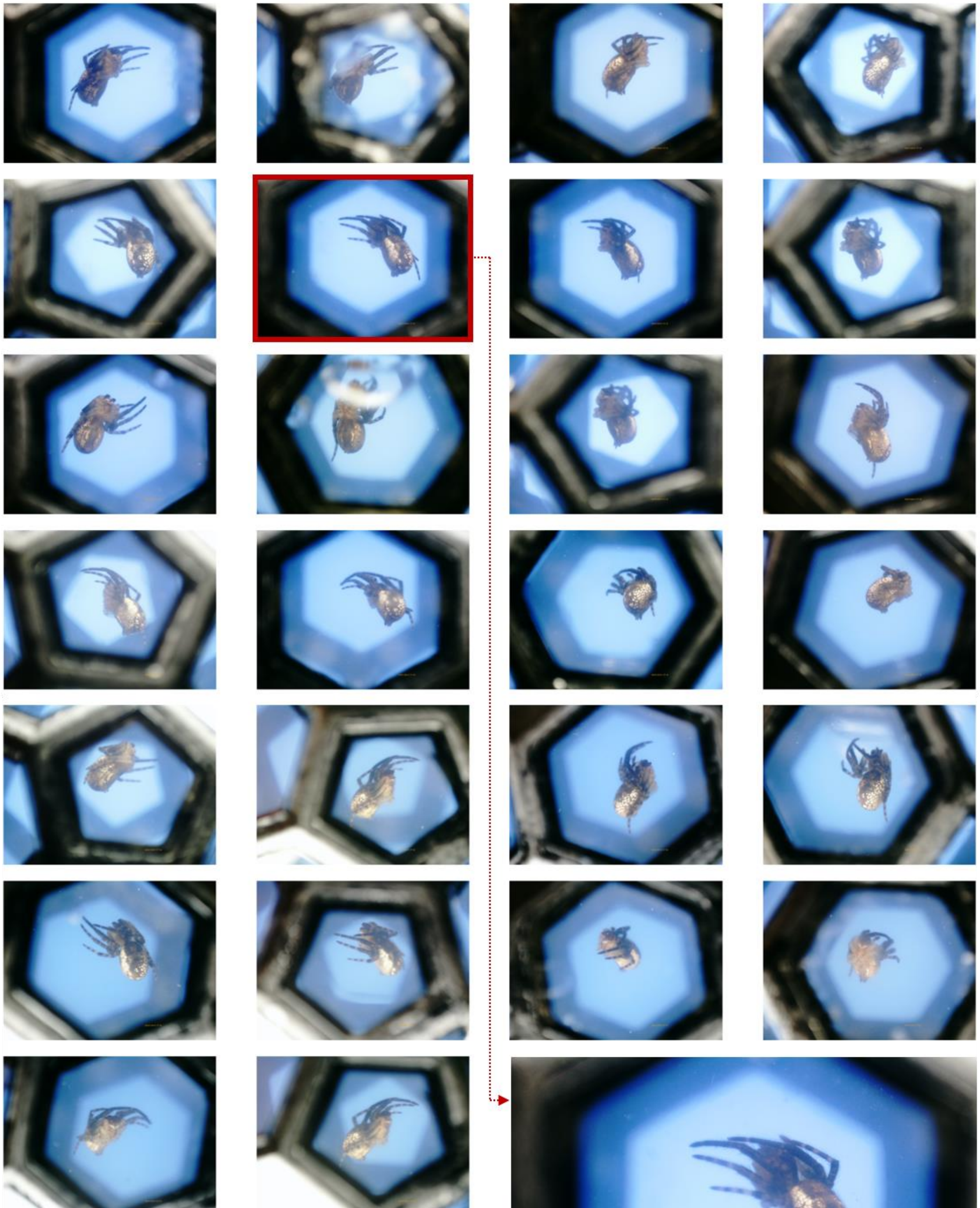

Figure 13. Multi-directional imaging from 26 angles using a hand-held digital microscope with the polyhedron-gimbal configuration. Although the polyhedron had 32 faces, six of those were dead angles (the attachment of the gimbal mechanism invalidated four faces, and an additional two were impractical due to the bulkiness of the gimbal). As seen above, a remaining large bubble impeded the observation for two angles. Overall, the spider could be observed from over 20 angles in all directions for the first time. Past mechanisms can rotate on one rotational axis but cannot observe top and bottom as a result [14].

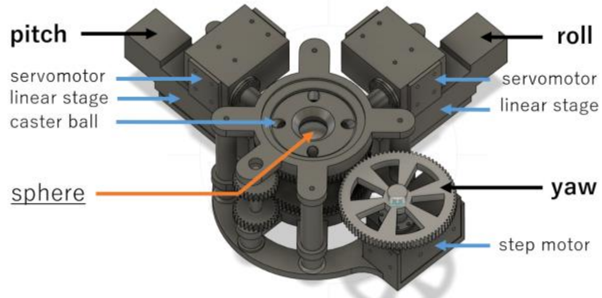

Figure 14. Overview of the sphere-friction model [15].

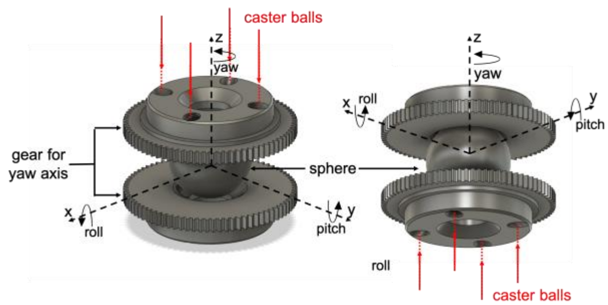

Figure 15. Mechanism of the yaw axis and caster ball system for the sphere-friction model, left: view of the top side caster balls; right: view of the bottom side caster balls.

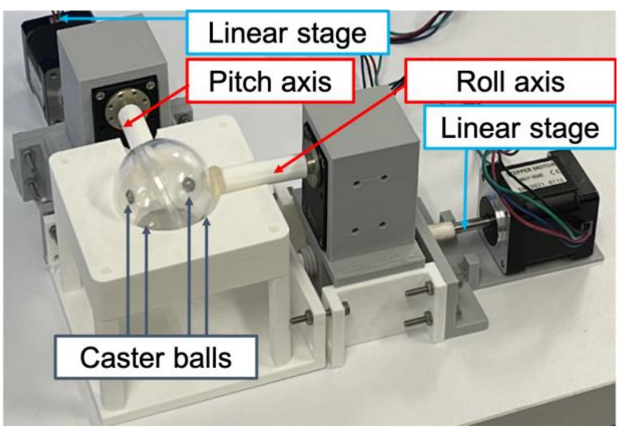

Figure 16. Mechanism design for the sphere-retractable axis model.

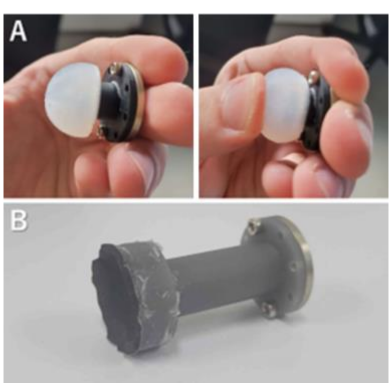

Figure 17. Optimization of the axis arm end to enhance friction [15].

A. Prototype building

Fig. 16 shows the initial prototype with only four caster balls at the bottom, so that the reader can better picture how the sphere is placed inside the mechanism. A lid is added with four additional caster balls to secure sphere's position, and the step motors were later replaced by servomotors.

This initial prototype was used to check the mechanism for the retractable pitch and roll and did not have a yaw axis. In particular, we spent some time optimizing the shape and material at the end of the axis arm which touches and moves the sphere. Indeed, for this mechanism to work, it is essential to minimize slippage. The following design principles are critical:

(1) The contact point to the sphere should match the sphere curvature to maximize contact surface and friction;

(2) The contact should neither be too loose (less friction) nor too tight (the sphere might be off-set, deformed, or break);

(3) The axis should not be off-set respective to the sphere;

(4) The sphere should have as few defects and irregularities as possible to avoid becoming stuck in the caster balls;

(5) The sphere should be as perfectly spherical as possible, to ensure that the friction force is constant throughout.

For point (1), we tested a spherical silicone rubber balloon with an empty air space. This balloon progressively adopted the shape of the target as it is pushed against it, as seen in **Fig. 17(a)**. However, this resulted in over 15° slippage over a travelled distance of 180° . Next, we tested a rigid end that fits the sphere's curvature, and coated it with 1.5 {mm}-thick silicone sponge anti-slipping material (GC100-1T) (see **Fig. 17(b)**). The final prototype is shown in **Fig. 18**.

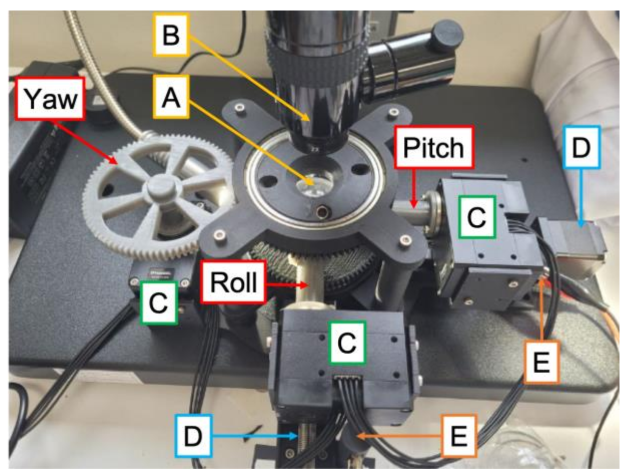

Figure 18. Final prototype showing the mechanis. A: sphere, B: digital microscope, C: servomotors, D: linear stages, E: limit switches for calibration [adapted from 15].

B. Software development

To control the mechanism, we developed custom software using Python, in the form of a Graphical User Interface (GUI) allowing simultaneous observation of the camera live feed and control of all three rotational axes (**Fig. 19**). The software is threaded to allow for multi-tasking, and a command-line interface (CUI) is also available for troubleshooting. Steps were taken to prevent data loss by checking the cache for unsaved data when the software launches.

Rotation Tab: this function implements quaternions to enable the translation of 2D mouse movement into 3D rotations. The user clicks and drags the spherical grid to rotate it. Clicking "Apply Rotation" prompts the mechanism to rotate the sphere in the physical world.

Tracking Tab: the user may set a region of interest (ROI) and keep track of this area on the live feed using CSRT, Channel and Spatial Reliability Tracking. If the area leaves the frame, the sphere is automatically rotated to place the target in the center of the frame. This tool returns an output displaying the target's trajectory around the sphere and a CSV table with the time-stamped polar coordinates.

Scanning Tab: automated scanning along a user-selected axis using time-lapse imaging. The "Frame by Frame" box allows the user to select the desired angle between each frame, and choose between automatic and semi-manual (manual focus) modes for scanning.

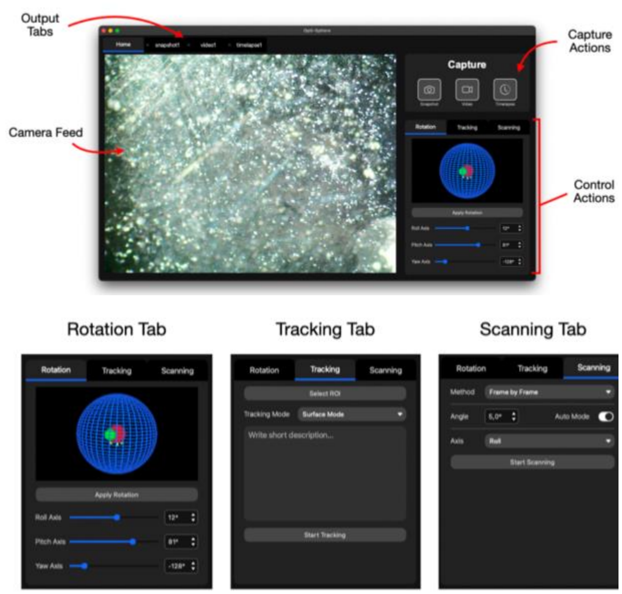

Figure 19. Custom-made software graphical interface [15].

C. Prototype evaluation

The specimen was encapsulated as described in SECTION III.B with some modifications. Notably, the sphere used here is a transparent plastic hollow ball of diameter 40 {mm} made of two hemispheres joined at the middle, creating a 3 {mm}-wide semi-blind spot at the equator. After a few tries, the encapsulation of a 3 {mm} clover leaf was successful (**Fig. 20**). **Fig. 21** shows the result of scanning along the pitch and roll axes, and a video is available (see Abstract).

Finally, the results of the evaluation for slippage along all three rotational axes are summarized in **Table 1**. In our experience, initial positioning of the sphere at the center of the caster balls to avoid any off-set with the pitch and roll axes is critical to avoid slippage.

Figure 20. 3 {mm} clover leaf placed in a transparent gel at the middle of a plastic sphere of diameter 40 {mm} [15].

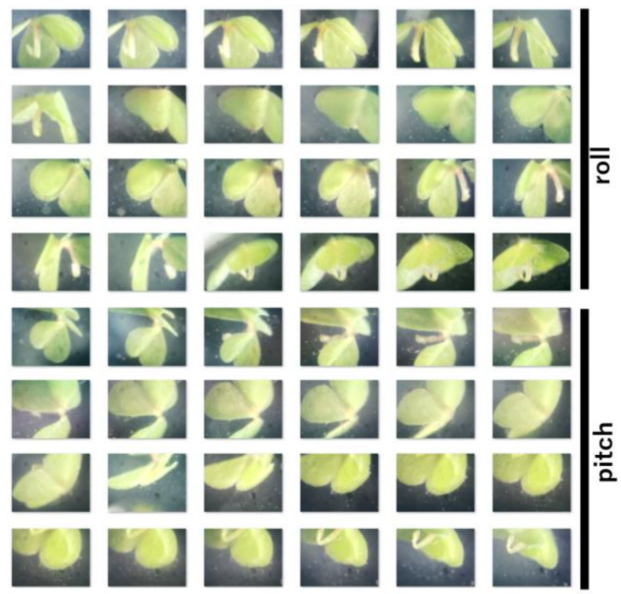

Figure 21. Result of automated scanning along the pitch and roll axes [15]. The width of one image is 4 {mm}.

TABLE I. ROTATIONAL AXES SLIPPAGE OVER 180°

Axis	Sphere material		t-test (n = 30)
	Plastic sphere[a]	***Glass sphere***[b]	***p-value***
Roll	3.72 ± 1.35	0.91 ± 0.61	<0.0001
Pitch	1.70 ± 0.97	1.93 ± 0.30	0.1677
Yaw[c]	0.09 ± 0.22		N.A.

a. Diameter: 40 {mm}, Weight: 32 {g}; b. Diameter: 40 {mm}, Weight: 40 {g}, c. The yaw axis is independent of sphere material and is not based on a friction mechanism

V. DISCUSSION AND FUTURE PERSPECTIVES

In this paper, we demonstrated the initial prototypes for a polyhedral or spherical microscope stage. This configuration has the advantage of realizing several types of analysis.

Firstly, the spherical configuration is expected to allow the tracking of a specimen crawling on the inside of the sphere, such as a snail or mollusk. Preliminary tests were done using a chiton, which is a species of marine mollusk; the tracking system is being optimized, and will be the subject of our next work. Similar systems have been developed with the animal walking on the outside of the sphere. In our case, the inside of the sphere lets us observe and quantify the movements of the bottom part of the animal, as well as make sure it stays in a controlled environment, with tuned parameters. In addition, in the case where the specimen is fixed at the center of the sphere using a transparent gel, our system should allow the tracking of specific parts of a structure as they move or grow, by changing the orientation of the sphere, or to measure the effect of gravity and/or centrifugal force on such growth by changing its orientation or spinning the sample.

Secondly, the spherical configuration should allow 3D photogrammetry from all directions for 3D reconstruction. At this time, we focused on demonstrating the mechanism of the actuated transparent sphere. As an initial test, in this paper, the imaging device was a simple digital microscope, but the compact design of our mechanism makes it compatible with any high end microscope with has a focal distance of > 2 cm. To test the scalability of our system, the 3D scanning function should be tested with calibration shapes of various sizes, ranging from the micrometer to the millimeter scale. The limitations depend almost entirely on the focal distance and width of the field of view of the selected microscope, which depends on the magnification.

Furthermore, to achieve 3D reconstruction, auto-focusing and/or stack imaging on the Z-axis is critical, highlighting the importance of combining our novel 3-rotational axis stage with standard XYZ linear stages for image acquisition. The full combination of all 6-DoF is under development and will be the subject of a future paper.

[1] T. Araki, "The history of optical microscope," in *Mechanical Engineering Reviews*, vol. 4, pp. 16-00242, 2017.

[2] N. Ogawa, H. Oku, K. Hashimoto, and M. Ishikawa, "Microrobotic Control of Paramecium Cells using Galvanotaxis," in Proceedings of the IEEE International Conference on Robotics and Biometrics, Hong Kong and Macau, pp. 23–25, 2005.

[3] H. Oku, M. Ishikawa, Theodorus, and K. Hashimoto, "High-speed autofocusing of a cell using diffraction patterns," in *Optics Express*, vol. 14, pp. 3952–3960, 2006.

[4] D. Krishnamurthy, H. Li, F. Benoit du Rey, P. Cambournac, A. G. Larson, and M. Prakash, "Scale-free vertical tracking microscopy," in *Nature Methods*, vol. 17, 1040–1051, 2020.

[5] R. Tomer, K. Khairy, F. Amat, P. J. Keller, "Quantitative high-speed imaging of entire developing embryos with simultaneous miltiview light-sheet microscopy", in *Nature Methods*, vol. 9(7): 755–763.

[6] J. Galipon and K. Tadakuma, "6-jiyūdo no tōmei kyūgata kenbikyō sutēji – 3D satsuei kanō na jittai kenbikyō no jitsugeni –," in the Proceedings of the *40th Annual Conference of the Robotics Society of Japan (RSJ2022)*, oral presentation in Japanese, Tokyo, 2022, non peer-reviewed.

[7] https://rechneronline.de/pi/geometry.php, accessed on Feb. 18, 2024.

[8] P. R. Cromwell, "Polyhedra," book published by Cambridge University Press, paperback edition, 451 p., 1999.

[9] H. W. Kroto, J. R. Heath, S. C. O'Brien, R. F. Curl, and R. E. Smalley, "C60: Buckminsterfullerene," in *Nature*, vol. 318 (6042): 162–163, 1985.

[10] N. G. Kim, J. S. Seo, H. G. Lim, J. S. Yoo, Y. A. Jung, Y. U. Seo, K. H. Yoo, "Control Method of Multipurpose Rollable Moving Device," US Patent US20200183410A1, 2019.

[11] K. Tadakuma and R. Tadakuma, "Mechanical Design of "Omni-Ball": Spherical Wheel for Holonomic Omnidirectional Motion," in *2007 IEEE International Conference on Automation Science and Engineering*, 2007.

[12] S. Ishida and H. Miyamoto, "Holonomic Omnidirectional Vehicle with Ball Wheel Drive Mechanism," in *Transactions of the Japan Society of Mechanical Engineers*, 2012.

[13] K. Abe, K. Tadakuma, and R. Tadakuma, "ABENICS: Active Ball Joint Mechanism With Three-DoF Based on Spherical Gear Meshings," in *IEEE Transactions on Robotics*, vol. 7, pp. 18061825, Apr. 2021.

[14] J. M. Girkin and M. T. Carvalho, "The light-sheet microscopy revolution," in *Journal of Optics*, vol. 20, pp. 053002, 2018.

[15] J. Galipon, A. Bordier, M. Duby, M. G. Selvamuthu, M. Imaizumi, R. Tadakuma, and K. Tadakuma, "Actuated Spherical Microscope Stage for Omnidirectional Vision," in the *Proceedings of the 24th Domestic Conference of the System Integration (SI) Division (SI2023)*, poster presentation in Japanese, Niigata, 2023, non peer-reviewed.